J Sol-Gel Sci Technol (2008) 48:315–321
DOI 10.1007/s10971-008-1824-y

ORIGINAL PAPER

Sol–gel synthesis and transport property of nanocrystalline $La_2Mo_2O_9$ thin films

Z. Zhuang · X. P. Wang · A. H. Sun · Y. Li · Q. F. Fang

Received: 25 February 2008 / Accepted: 1 August 2008 / Published online: 13 August 2008

Abstract $La_2Mo_2O_9$ films were successfully synthesized on silicon (100) and poly-alumina substrates via modified sol–gel method with inorganic salts of $La(NO_3)_3$ and $(NH_4)_6Mo_7O_{24}$ as precursors. Pure $La_2Mo_2O_9$ phase was confirmed by XRD if the annealing temperature was higher than 500 °C. Energy dispersive spectrometry (EDS) of TEM revealed that the molar ratio of La to Mo was nearly 1:1. Field-emission SEM characterization showed that the films were dense, crack-free and uniform. The grain size of the films ranged from 30 to 400 nm depending upon the calcination temperature and duration time. The roughness calculated from AFM topography varied in the range between 10 and 35 nm. The thickness of the films was more than 200 nm for single-layered films. The electrical conductivity of the films reaches 0.06 S/cm at 600 °C that was almost more than one order of magnitude higher than that of the corresponding bulk material.

Keywords Sol–gel chemistry · $La_2Mo_2O_9$ ionic conductors · Thin films · Inorganic salts

1 Introduction

The development of intermediate temperature solid oxide fuel cells (SOFC) and oxygen sensors are an important step towards commercialization of oxide ionic conductors [1–10]. As an essential requirement of SOFC and oxygen sensors, thin layers of electrolyte can minimize the ohmic loss across the electrolyte and increase power efficiency, which will make SOFC operate at lower temperatures, lower the system cost, and facilitate wide application of SOFC. Therefore it is of great importance to synthesize dense, crack-free, and homogeneous films of oxide ionic conductors. In another side, searching for new superior electrolytes with outstanding electrical conductivity is another promising way to decrease operating temperature of SOFC and other oxygen ionic devices. The newly discovered $La_2Mo_2O_9$ system has attracted much attention owing to its high oxide ionic conductivity (0.06 S/cm at 800 °C) [1–3]. Its vacancy–deficient nature, which was thought as the origin of high electrical conductivity, is different from the widely investigated oxide ionic materials such as doped CeO_2 [11–14, 15], ZrO_2 [11, 15–18] or $LaGaO_3$ [19–21] where the oxygen vacancies were introduced through doping with lower valence elements.

Recently, a considerable enhancement of ionic conductivity in nanocrystalline CeO_2 [11, 12], $SrCe_{0.95}Yb_{0.05}O_3$ [13, 14], $(RE_2O_3)_{0.08}(ZrO_2)_{0.92}$ (RE=Sc,Y) [17, 18] thin films on silicon or poly-alumina were reported, and the enhancement was related to the decrease of grain boundary resistance. Hence it is a feasible and practical way to synthesize nanocrystalline thin films for the application of electrical devices. Nevertheless, most researches of $La_2Mo_2O_9$ system are focused on bulk materials instead of films. To our knowledge, there is only one reference in the literature that reported the fabrication of $La_2Mo_2O_9$ thin films [22], where the thin films were prepared on porous Al_2O_3 substrate by RF sputtering method. As described there [22], it is difficult to control the composition of films and to fabricate relatively thick films via RF sputtering method.

Z. Zhuang · X. P. Wang · A. H. Sun · Q. F. Fang (✉)
Key Laboratory of Materials Physics, Institute of Solid State Physics, Chinese Academy of Sciences, Hefei 230031, People's Republic of China
e-mail: qffang@issp.ac.cn

Y. Li · Q. F. Fang
Ningbo Institute of Material Technology and Engineering, Chinese Academy of Sciences, Ningbo 315040, People's Republic of China

As well known, sol–gel method can synthesize thin films in open air according to accurate original stoichiometric ratio at relatively low temperature over the other fabrication methods. In this paper, a modified Pechini-type sol-gel method via inorganic salts was developed to fabricate dense, thick and crack-free nanocrystalline $La_2Mo_2O_9$ thin films on silicon (100) and polycrystalline alumina at relatively low temperature, and the densification process of the $La_2Mo_2O_9$ films was discussed. The electrical conductivity of $La_2Mo_2O_9$ films was enhanced by more than one order of magnitude in comparison with the bulk materials.

2 Experimental process

2.1 Sample fabrication

The sol was prepared in open air with $La(NO_3)_3{\cdot}6H_2O$ (purity ≥99.95%), and ammonia complexed molybdic acid, $(NH_4)_6Mo_7O_{24}{\cdot}4H_2O$ (≥99%) as raw materials. Firstly, an appropriate amount of $(NH_4)_6Mo_7O_{24}{\cdot}4H_2O$ was dissolved in 20 ml ethylene glycol (designated as EG) with nitric acid, then the corresponding molar mass $La(NO_3)_3{\cdot}6H_2O$ was poured into the above beaker with nitric acid and then a transparent solution was obtained by vigorous stirring. After that, an appropriate amount of citric acid (designated as CA) was added in order to avoid precipitation and to chelate cation ions [18, 23, 24]. Finally, the solution was heated to a temperature between 70 and 90 °C in order to evaporate redundant solvent to form 10 mL viscous sol. This yellow sol was stocked at room temperature for at least 24 h for further esterification between CA and EG. From the as-prepared sol, the wet films were deposited onto Si(100) and Al_2O_3 substrates with a spin-coating speed of about 3,500 rpm and a period of about 60 s. The wet films were dried at 120 °C, and then preheated and annealed at temperature ranging from 350 to 450 °C for several minutes and 500 to 700 °C for several hours by the means of rapid thermal annealing [25, 26]. The above procedures can be repeated to fabricate thicker films.

2.2 Characterization methods

The gel (dried at 100 °C for 30 min) decomposition behavior was investigated with a thermal analyzer (Pyris Diamond DSC, Perkin-Elmer Co., US) in air with a heating rate of 10 °C/min by using α-Al_2O_3 as a reference. A Philips X'pert PRO X-ray diffractometer (XRD) was used to detect the films structure at different calcination temperature and duration time on Si and Al_2O_3 substrates. The gel annealed at 550 °C for 10 h was used for the stoichiometry analysis by Energy dispersive spectrometry (EDS) equipped in a transmission emission microscopy (TEM) of JEOL Company. The flat figures and cross-section of films were characterized by field-emission scan electron microscopy (FE-SEM) of Oxford Instrument Company. An AutoProbe CP atomic force microscopy (AFM) of Veeco Instrument Co. was employed to compare the roughness of films in different annealing situations.

2.3 Electrical conductivity measurements

The electrical property of a film deposited on the alumina substrate (annealed at 650 °C for 10 h, 150 nm) was determined using alternative current (AC) impedance measurement by two-probe method from 400 to 620 °C in air on Hioki 3531 Z Hi-Tester with a frequency range from 50 Hz to 5 MHz. The maximum applied ac voltage is about 0.5 V. With Ag paste, two Pt lead electrodes were adhered to two cross sections (0.5 cm × 0.03 cm) of the film with an interelectrode area of 0.7 cm × 0.5 cm, and then the paste was fired at 650 °C for 30 min. After each change in temperature the specimen was allowed to equilibrate for at least 30 min before the next measurement was taken. This configuration of electrodes is similar to the one adopted in the characterization of bulk conductivity for doped ZrO_2 films [17, 18]. The corresponding bulk material was prepared according to the above sol–gel procedure (annealing at 850 °C, 2–4 μm of average grain size) for comparison in electrical conductivity [27].

3 Results and discussion

3.1 Phase formation and grain size

The XRD patterns presented in Fig. 1a show that pure $La_2Mo_2O_9$ phase was obtained when the annealing temperature is above 500 °C. Compared to the bulk materials prepared by solid-state reaction method in which the lowest calcination temperature must be beyond 900 °C to obtain a pure phase, the films prepared by sol–gel method can lower the calcination temperature as many as 400 °C. From the Debye-Sherrer formula, the average grain size of the film can be estimated as 30 nm when the film was annealed at 500 °C for 10 h, which increases to 60 and 150 nm when the films were annealed at 600 °C for 10 h and at 700 °C for 5 h, respectively. Since the coarse surface of alumina serves as crystallization nuclei, the films deposited on alumina always exhibit bigger grain than that on silicon at the same annealing condition. From Fig. 1a one can estimate the average grain size of the films deposited on Al_2O_3 as 100 nm when annealed at 600 °C for 10 h and 400 nm when annealed at 700 °C for 5 h, respectively. Similarly, long annealing time also leads to bigger grain as presented in Fig. 1b. The grain size of the film deposited on silicon

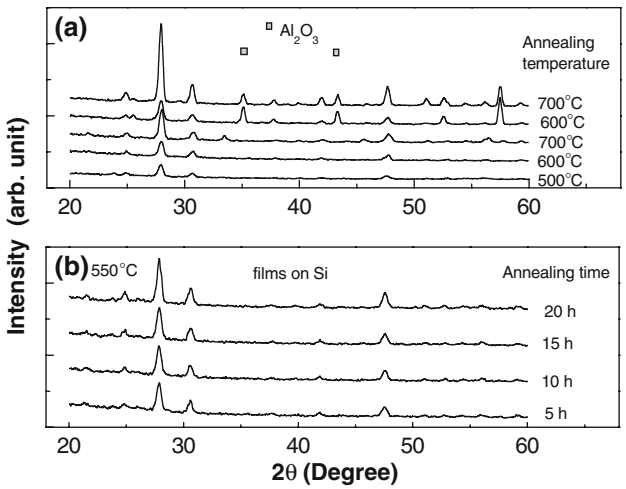

Fig. 1 XRD patterns of $La_2Mo_2O_9$ films (**a**) deposited on silicon (the first three curves from bottom) and on Al_2O_3 (the last two curves from bottom) with different annealing temperatures and (**b**) deposited on silicon and annealed at 550 °C for different annealing time

Table 1 The elements composition of $La_2Mo_2O_9$ gel annealed at 550 °C for 10 h

Element	Weight%	Weight% sigma	Atomic%
C K	3.68	0.31	15.00
O K	13.97	0.21	42.69
Cu K	24.48	0.18	18.84
Mo K	19.66	0.24	10.02
La L	38.21	0.26	13.45
Total	100.00		

and annealed at 550 °C grows from 25 to 45 nm when calcination time was prolonged from 5 to 20 h.

From the EDS analysis results listed in Table 1, it can be seen that five elements were detected in the fired gel: carbon, copper, oxygen, molybdenum, and lanthanum. The carbon was left from the inorganic solvent and the signal of copper was from the sample holder. The molar ratio between La, Mo, and O is about 1.3:1:4.3. Taking into account the large measurement error of the EDS method, it can be concluded approximately that the La, Mo, and O are stoichiometric as $La_2Mo_2O_9$.

3.2 Annealing method

As well known, the preheating temperature and annealing method have critical effects on the film quality. In order to determine the optimum conditions of thermal treatment, thermal gravimetric (TG) measurement was exploited in this study, as shown in Fig. 2. It can be seen that besides a small weight loss centered at about 80 °C owing to the

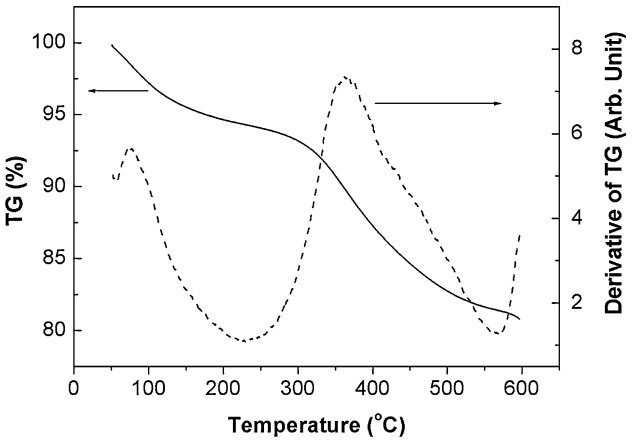

Fig. 2 TG curves of $La_2Mo_2O_9$ gel dried at 100 °C for 30 min (solid line) and the corresponding derivative (dash line)

evaporation of absorbed water and remained organic solvent, a clear drop of weight loss centered at about 360 °C appears, indicating that the gel completely decomposes above 500 °C and starts to crystallize into $La_2Mo_2O_9$ phase, which agrees well with the XRD results. Below 350 °C, a great deal of organic impurities is left in the as-preheated thin film. When such-dealt thin film is annealed at higher temperature, the organic impurities will be promptly burnt out to release gases, which usually results in pinholes and cracks [18]. Therefore, the preheated temperature must be above 350 °C since fewer impurities left will make the film more crack-free.

In another side, the conventional furnace annealing (CFA), which gradually increases the temperature of the samples, prefers crystallization to densification [25]. Therefore the film with porous structure rather than dense one is generally resulted by CFA method. In addition, the release of internal stress in CFA process usually results in cracks as temperature increases. Taking calcination temperature of 600 °C as an example, three samples annealed with CFA method were shown in Fig. 3a, where the heating rate was 1, 3, and 10 °C/min, respectively. In the cases of low heating rate, giant cracks were generated in the annealing process. When the heating rate was increased to 10 °C/min however, no cracks appeared and only small superficial holes were detected. This fact prompts us that high heating rate can be helpful to retard the development of cracks in the films. So rapid thermal annealing (RTA) method, in which the samples are rapidly put into the furnace that was kept at a constant high temperature, was employed on account of its obvious advantage of prompt densification process, localization of the internal stress and block of the crack formation [25, 26].

Residual stress could be released in further post annealing. However, as shown in Fig. 3b, at a low preheating temperature such as 350 °C, the gel shrinkage was

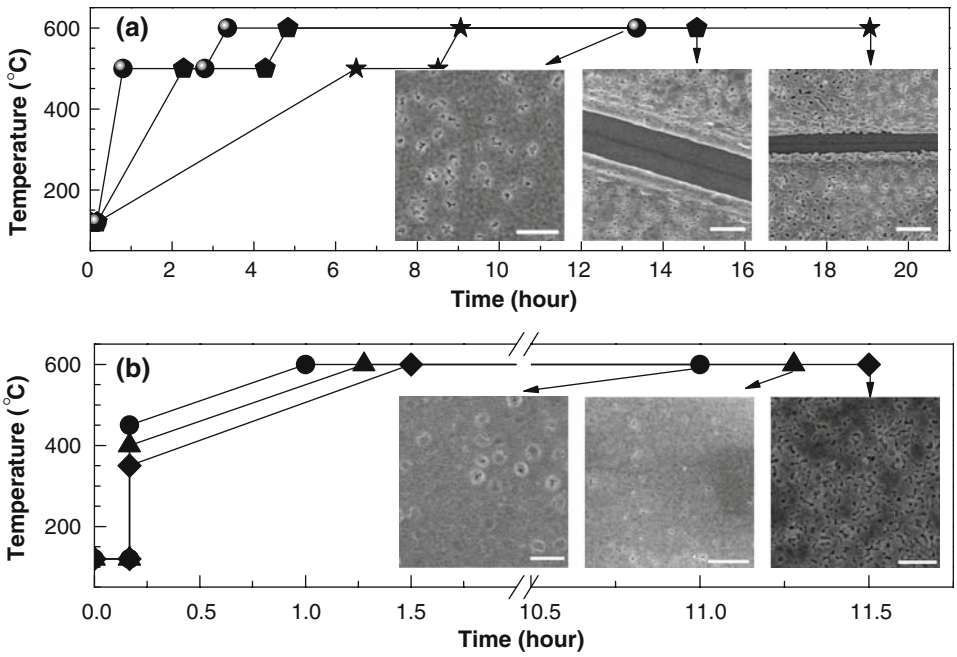

Fig. 3 Film morphology (scale unit of 1 μm) of films annealed via different annealing methods: (**a**) Conventional furnace annealing (CFA): three films were heated from 120 to 500 °C with a heating rate of 1 °C/min (stars), 3 °C/min (pentagons), and 10 °C/min (balls), respectively, then annealed at 500 °C for 2 h, and at last heated to 600 °C with a heating rate of 3 °C/min and annealed at 600 °C for 10 h. (**b**) Rapid thermal annealing (RTA): three films were rapidly heated to 350 °C (diamond), 400 °C (triangle), and 450 °C (circle), respectively, at last heated to 600 °C with a heating rate of 3 °C/min and annealed at 600 °C for 10 h

not enough for densification and porous structure was resulted. On the other hand, preheating at above 450 °C often resulted in prominences owing to prompt release of gases. Therefore dense, crack-free, uniform $La_2Mo_2O_9$ films can be produced on silicon substrate when the gel was preheated at about 400 °C for several minutes by RTA method and then post-annealed at temperature ranging from 500 to 700 °C by CFA with a heating rate of 3 °C/min. In Fig. 3b the results at the post-annealed temperature of 600 °C for 10 h are shown as an example.

The average grain size of the film is about 40 nm when the film was post-annealed at 550 °C for 10 h, as estimated from the SEM picture shown in Fig. 4a. Figure 4b–d present the SEM pictures of the films post-annealed at 650 °C for 10 h, 700 °C for 5 h, and 700 °C for 10 h, and the corresponding average grain size is about 100, 150, and 200 nm, respectively, which agrees well with the calculation from the XRD results. From Figs. 4c and 5d, one can find that higher annealing temperature and long time lead to not only bigger grain but rougher surface. As shown in Fig. 4e, f, the grain size of the film grows to 150 and 400 nm when the film was deposited on alumina substrate and post-annealed at 650 °C for 10 h and 700 °C for 5 h, respectively.

From the AFM topography shown in Fig. 5, it can be seen that the film deposited on Si substrate is dense and relatively flat when it was post-annealed at 550 °C for 10 h, and its R_{rms} value (root-mean-square roughness) is about 10 nm. The R_{rms} values increase when the post-annealing temperature increases, as listed in Table 2. However, the highest R_{rms} value is about 35 nm when the film was post-annealed at 700 °C for 10 h, which is much smaller than the thickness of the film (about 500 nm).

3.3 Optimization of sol preparation

During the sol preparation both concentration and viscosity are two important factors to ensure that a suitable amount of sol remains on the substrates after spin coating and supplies enough precursor to form dense films. If the concentration and viscosity of sol are too low, the process of spin coating, drying, preheating, and annealing must be repeated several times in order to get relatively dense and thick film, which is a time- and energy-consuming procedure [18]. More importantly, pinholes are usually generated in dozens of such repetitive spin-coating processes. Figure 6a shows the SEM picture of a sample synthesized from the 0.1 M sol following the above sample fabrication procedure (spin coated with 3,500 rpm, then dried at 120 °C, preheated at 400 °C and annealed at 600 °C for 10 h, respectively). It can be seen that in this case there are only isolated dots on the substrate. As the sol concentration increases to 0.2 M, the film is connected but lots of large pores still remain, as exhibited in Fig. 6b. When the sol concentration increases to 0.4 M the film becomes dense enough, as shown in Fig. 6c. In this case however, cracks appear in the film owing to the large thickness of the film and the mismatch of thermal expansion coefficient between the Si substrate and the film. Therefore, the concentration of sol is chosen as 0.3 M.

In the Pechini-type sol–gel process [23, 24], CA is often used as ligand to coordinate with the metal ions and to avoid hydrolyzation and precipitation. Sometimes ethylene glycol (EG) is used as assistant ligand. In the present case, EG was chosen as solvent while CA as ligand, since $La(NO_3)_3$ and $(NH_4)_6Mo_7O_{24} \cdot 4H_2O$ can dissolve in EG

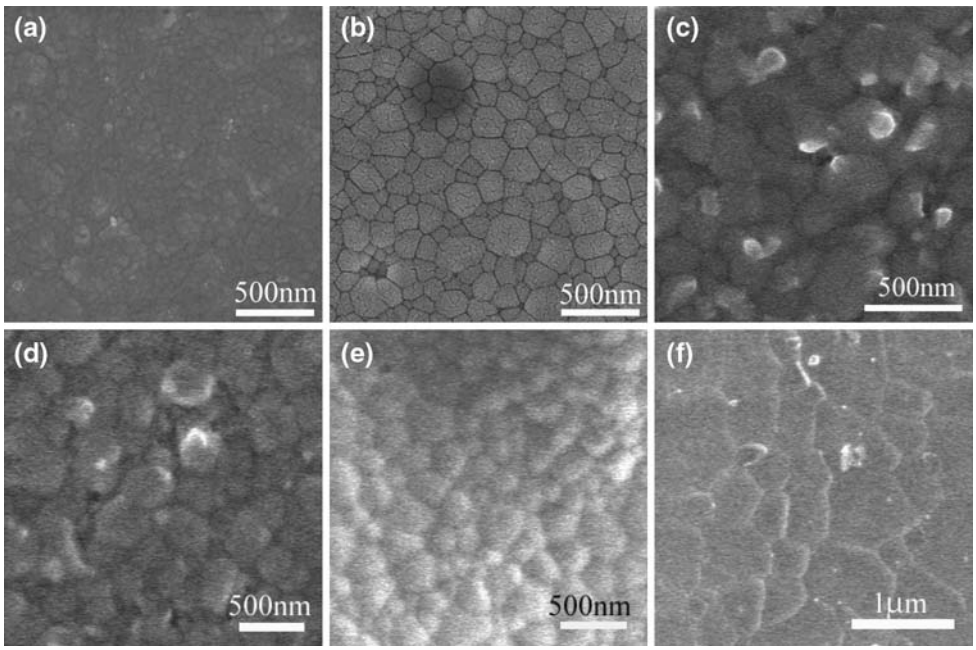

Fig. 4 FESEM images of $La_2Mo_2O_9$ films annealed (**a**) at 550 °C for 10 h, (**b**) at 650 °C for 10 h, (**c**) at 700 °C for 5 h, and (**d**) at 700 °C for 10 h on Si substrate. (**e**) and (**f**) are the films annealed at 650 °C for 10 h and 700 °C for 5 h on Al_2O_3, respectively

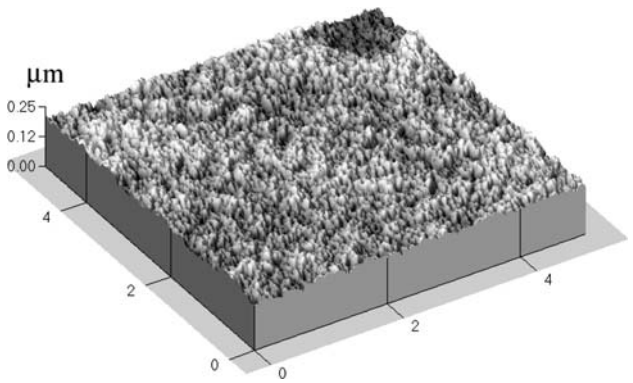

Fig. 5 AFM topography of the film annealed at 550 °C for 10 h on silicon substrate

Table 2 R_{rms} values for $La_2Mo_2O_9$ films deposited on Si(100) annealed at different temperature for 10 h

Samples no.	1	2	3	4
Annealing temperature (°C)	550	600	650	700
R_{rms} (nm)	10	17	27	35

easily but hardly coexist steadily in acid surrounding for long time without CA. In this case, CA not only serves as ligand but also participates in esterification reaction with EG to form viscous polymerized sol. Therefore, the molar ratio of CA: cation ion (denoted as CI, including La^{3+} and Mo^{6+}) can be used to control the viscosity of the sol. When the CA/CI ratio in the sol is less than 1, porous film was synthesized as shown in Fig. 7a since the esterification reaction is too deficient to form polymerized viscous sol. On the other hand, too much CA/CI ratio would introduce redundant organic impurities that result in cracks or pinholes in the film during the annealing process at high temperature, as shown in Fig. 7c. Hence dense films can be synthesized if the CA/CI ratio was controlled in the range from 2 to 1 and the viscosity of the sol was correspondingly in the range from 1,200 to 1,800 MPa s, as shown in Fig. 7b.

From the above attempts, one can conclude the optimal procedure for synthesis of dense $La_2Mo_2O_9$ nanocrystalline films as followings. At first 0.03 M $La_2Mo_2O_9$ precursor (consisting of $La(NO_3)_3$ and $(NH_4)_6Mo_7O_{24}$) is dissolved in 20 mL ethylene glycol with nitric acid, then citric acid is added according to CA/CI molar ratio in the range from 2 to 1. Finally the sol is heated between 70 and 90 °C to form 10 mL viscous sol. After spin coating with 3,500 rpm, the wet gel was dried at about 120 °C for several minutes, and then preheated at 400 °C for several minutes by RTA method and then post-annealed at temperature ranging from 500 to 700 °C until the films become dense.

Figure 8a is the SEM picture of a single-layered film deposited on silicon from such sols and then post-annealed at 550 °C for 10 h. It can be seen that the thickness of the film is about 200 nm and the film adheres to the substrates firmly. It is easy to fabricate thicker film by repeating the above process several times. The thickness of a three-layered film (550 °C for 10 h) is about 750 nm, as exhibited in Fig. 8b. But for films deposited on alumina, it is hard to make continuous and flat single-layered film because of the rougher surface of alumina. Three-layered and six-layered films annealed at 650 °C for 10 h with thickness of 680 nm and about 1 μm, as shown in Fig. 8c, d, respectively, can cover the coarse surface of Al_2O_3 wholly and exhibit dense, continuous and flat surface.

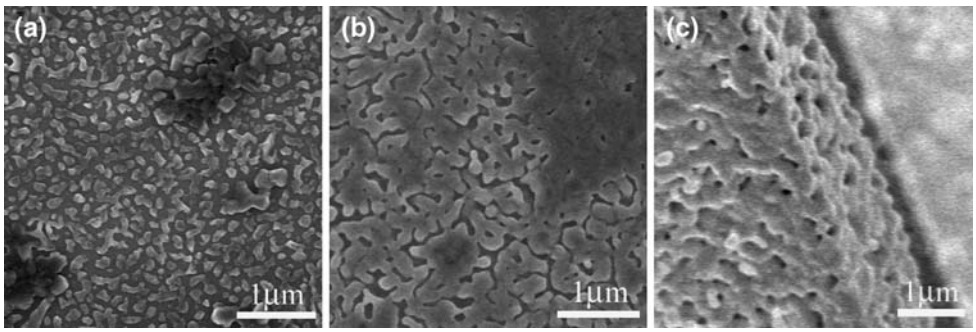

Fig. 6 FESEM images of $La_2Mo_2O_9$ films (spin-coated with 3,500 rpm, then dried at 120 °C, preheated at 350 °C and annealed at 600 °C for 10 h, respectively) synthesized from different concentration sols: (**a**) 0.1 M, (**b**) 0.2 M, and (**c**) 0.4 M

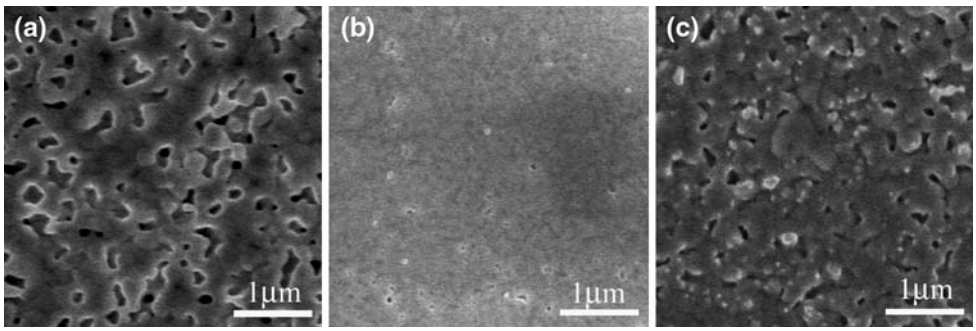

Fig. 7 SEM graphs of films synthesized from the sols with different ratios of CA to cation ions: (**a**) <1, (**b**) between 1 and 2, and (**c**) >2

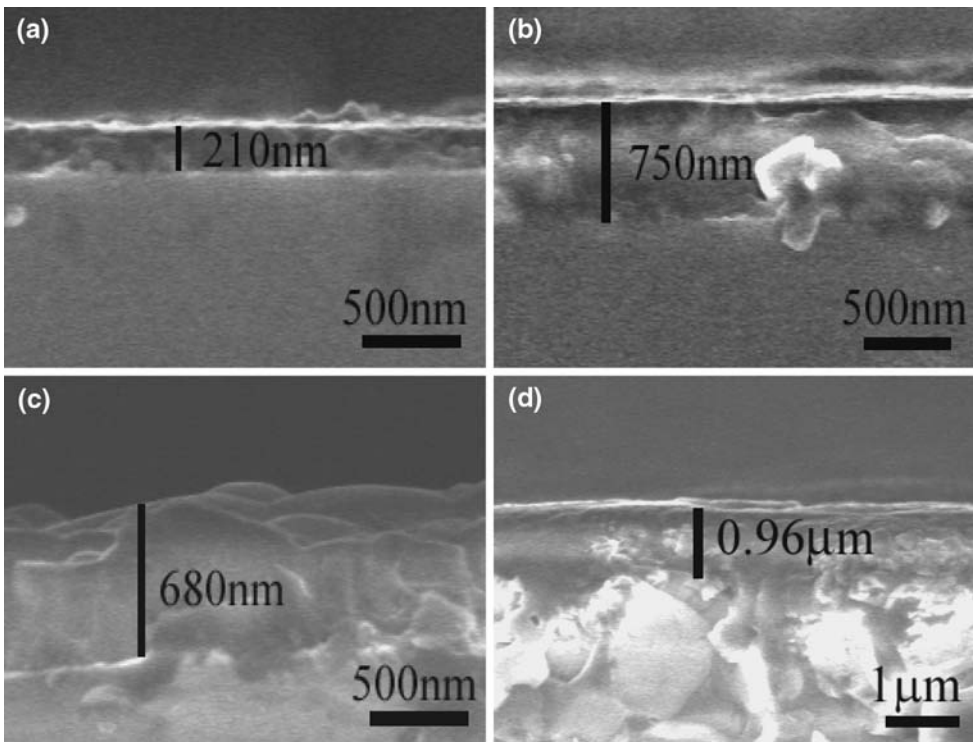

Fig. 8 Cross section images of $La_2Mo_2O_9$ films: (**a**) single-layered, and (**b**) three-layered on silicon (annealing at 550 °C for 10 h), (**c**) three-layered, and (**d**) six-layered on Al_2O_3 (annealing at 650 °C for 10 h)

3.4 Electrical conductivity

The thermal dependence of electrical conductivity of a dense $La_2Mo_2O_9$ nanocrystalline film deposited on alumina (post-annealed at 650 °C for 10 h, as shown in Figs. 4e and 8d for the topography and cross section picture, respectively) is given in Fig. 9 as an example, where the data of a bulk material [27] are shown for comparison. It is obvious that the conductivity curve of the nanocrystalline thin film embodies its α/β phase transition at 580 °C as previously reported in bulk materials [1, 3, 27]. Furthermore, electrical conductivity of the films is enhanced in

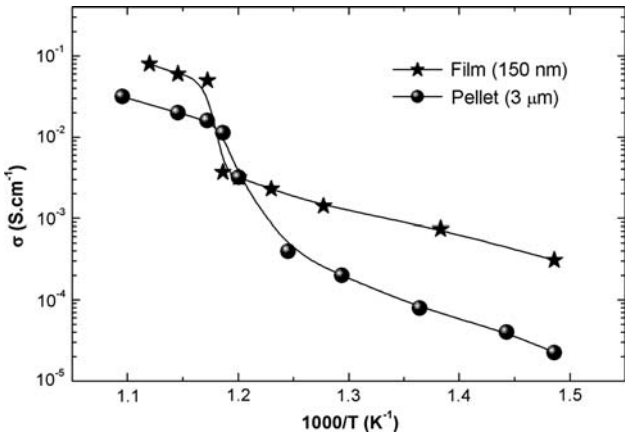

Fig. 9 Temperature dependence of electrical conductivity of $La_2Mo_2O_9$ nanocrystalline thin film (star) deposited on Al_2O_3 (annealed at 650 °C for 10 h, 150 nm) and bulk materials prepared by sol–gel method (ball)

comparison with the bulk materials synthesized by sol–gel method. For example, the electrical conductivity at 600 °C of the films reaches 0.06 S/cm, which is similar to the conductivity of ZrO_2:16%Y film [11] but half order of magnitude higher than that of the pellet prepared by sol–gel method (3 μm in grain size). As determined from the slope of the lines below 580 °C, the activation energy of conductivity of nanocrystalline film is about 0.67 eV, which is much smaller than that of pellets (about 1.0 eV) synthesized by sol–gel method [27] and by freeze-dried precursors [28]. This enhancement in conductivity can be ascribed to the decrease of grain boundary resistance when the grain size reduces to the nanometer regime, since the interfacial effects of grain boundaries may become prominent and the decrease of size-dependent grain boundary impurities segregation and defect formation energy would facilitate oxide ion transport across or along the grain boundaries [20–22, 27]. However, the effect of space-charge on resistance that is dominant in doped CeO_2 thin film [11], is not important in the $L_2Mo_2O_9$ system because the oxide ions in the $L_2Mo_2O_9$ system diffuse via intrinsic oxygen vacancy instead of the one introduced by doping, and thus much less space charges exist along grain boundary.

4 Conclusion

In summary, dense, crack-free, and homogeneous nanocrystalline $La_2Mo_2O_9$ thin films on silicon (100) and polyalumina substrate have been successfully fabricated by modified sol-gel method. Citric acid was used to take part in chelation reaction with metal ions and esterification reaction with ethylene glycol. These would keep sol steady and homogeneity for preservation. Moreover, spin coating of the concentrated and viscous sol shows its advantage of easily fabricating dense, crack-free and thick films at reduced annealing temperature. The as deposited film exhibits a notable enhancement in electrical conductivity at whole temperature range. That will be very useful to understand the source of ionic conduction enhancement and fabricate good performance electrical devices.

Acknowledgements This work has been subsidized by the National Natural Science Foundation of China (Grant No.50672100, 50702061), Ningbo Civic Natural Science Foundation (Grant No.2006A610057), Ningbo Civic Project of International Cooperation (Grant No.2006 B100080), and Zhejiang Provincial Project of International Cooperation (Grant No.2007C24022).

References

1. Lacorre P, Goutenoire F, Bohnke O, Retoux R (2000) Nature 404:856
2. acorre P (2000) Solid state science 2:755
3. Goutenoire F, Isnard O, Lacorre P (2000) Chem Mater 12:2575
4. Wang XP, Fang QF (2002) Phys Rev B 65:06304
5. Khadasheva ZS, Venskovskii NU, Safronenko MG, Mosunov AV, Politova ED, Stefanovich SY (2002) Inorg Mater 38:1381
6. Rocha RA, Muccillo EN (2003) Chem Mater 15:4268
7. Georges S, Goutenoire F, Altorfer F, Sheptyakov D, Fauth F, Suard E, Lacorre P (2003) Solid State Ionics 161:231
8. Tsui D, Hsieh M, Tseng J, Lee H (2005) J Eur Ceram Soc 25:481
9. Wang XP, Fang QF (2002) Solid State Ionics 146:185
10. Wang XP, Fang QF, Li ZS, Zhang GG, Yi ZG (2002) Appl Phys Lett 81:3434
11. Tian C, Chan SW (2002) J Am Ceram Soc 85:2222
12. Chiang YM, Lavik EB, Kosacki I, Tuller HL, Ying JY (1996) Appl Phys Lett 69(2):186
13. Kosacki I, Anderson HU (1996) Appl Phys Lett 69:4171
14. Kosacki I, Anderson HU (1997) Solid State Ionics 97:429
15. Hui S, Roller J, Yick S, Zhang X, Decès-Petit C, Xie Y, Maric R, Ghosh D (2002) J Power Sources 172:493
16. Gao X (1997) Solid State Ionics 96:247
17. Zhang YW, Jin S, Yang Y, Li GB, Tian SJ, Liao CS, Yan CH (2000) Appl Phys Lett 77:3409
18. Zhang YW, Yang Y, Jin S, Tian SJ, Li GB, Jia JT, Liao CS, Yan CH (2001) Chem Mater 13:372
19. Ishihara T, Kilner JA, Honda M, Takita Y (1997) J Am Chem Soc 119:2747
20. Ishihara T, Akbay T, Furutani H, Takita Y (1998) Solid State Ionics 113–115:585
21. Pelosato R, Natali Sora I, Ferrari V, Dotelli G, Mari CM (2004) Solid State Ionics 175:87
22. Laffez P, Chen XY, Banerjee G, Pezeril T, Rossell MD, Von Tendeloo G, Lacorre P, Liu JM, Liu ZG (2006) Thin Solid Films 500:27
23. Pechini MP (1967) US Patent 3,330,697, 11 July
24. Kuang WX, Fan YI, Yao KW, Chen Y (1998) J Solid State Chem 354:140
25. Scherer GW (1997) J Sol-Gel Sci Tech 8:353
26. Scherer GW, Calas S, Sempéré R (1998) J Sol-Gel Sci Tech 13:937
27. Wang JX, Wang XP, Liang FJ, Cheng ZJ, Fang QF (2006) Solid State Ionics 177:1437
28. Marrero-López D, Ruiz-Morales JC, Núñez P, Abrantes JCC, Frade JR (2004) J Solid State Chem 177:2378